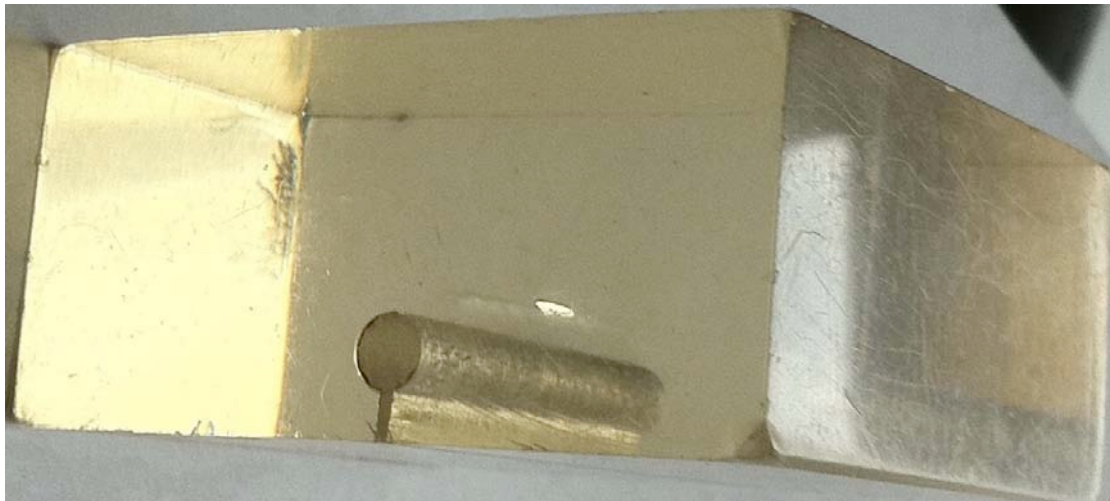
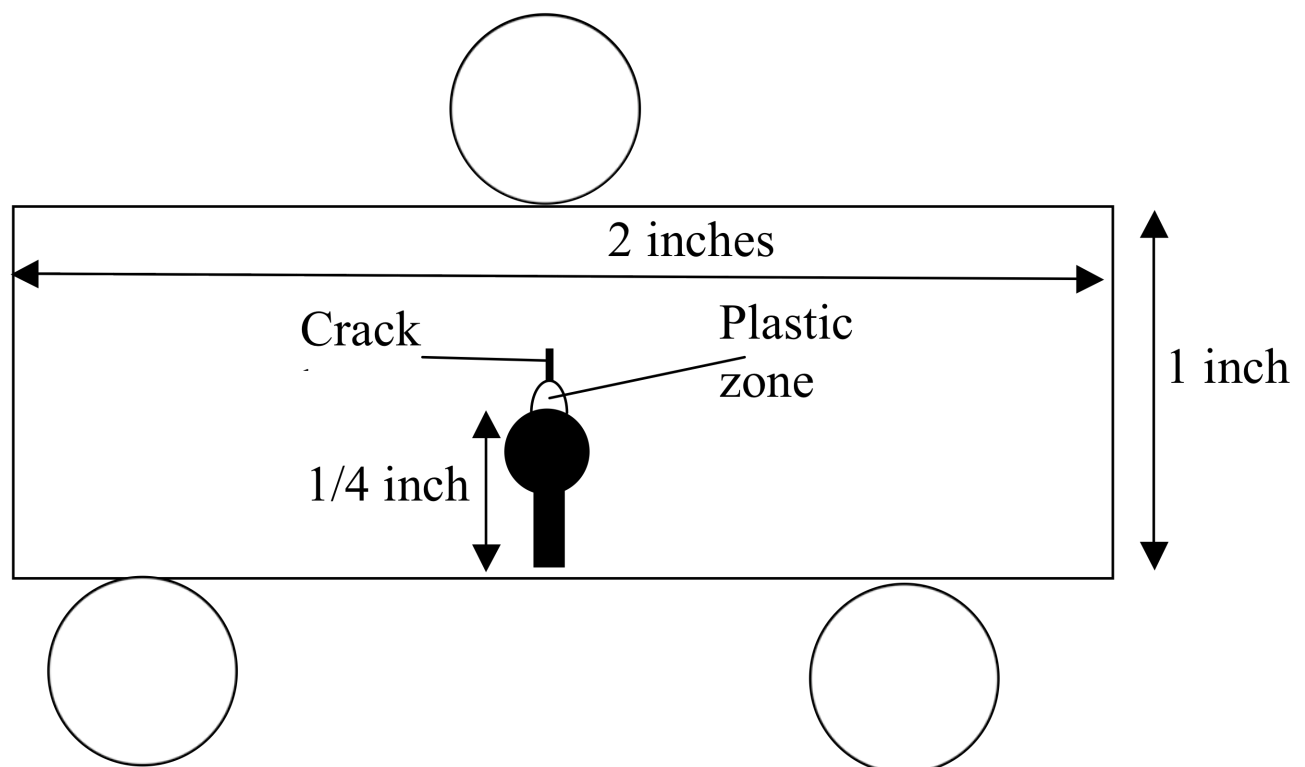


Brittle Crack Initiation at the Elastic-Plastic Interface

Experiments by Bernard Schaeffer
Post-doc at Syracuse University, 1968-69



Polycarbonate block with a notch made from a hole. It was bent in three point bending. The tensile fiber is on the bottom.



Brittle Crack Initiation at the Elastic-Plastic Interface

A. M. GARDE AND V. WEISS

To study fracture initiation near notches experiments were conducted on polycarbonate at room temperature. It could be demonstrated conclusively that cracks are nucleated under the influence of a critical normal stress at the elastic-plastic boundary. Slip line field theory allows the determination of the critical normal fracture stress from the knowledge of the notch root radius and the location of the crack nucleation. For 0.5 in. thick specimens with root radii between 0.001 and 0.01 in. the calculated critical fracture stress of polycarbonate is nearly constant, 21.2 ± 0.6 ksi. An analysis of the data in accordance with the theory developed by R. Beeuwkes, Jr. for parabolic notches resulted in critical fracture stress values of approximately 21.5 ksi. Specimens with central holes between 0.04 and 0.05 in. diam also showed crack nucleation below the surface of the hole but the calculated critical fracture stress values were considerably lower, approximately 11.2 ksi. This may be attributed to the loss of plane strain conditions in these 0.5 in. thick specimens. The experimentally observed slip lines in polycarbonate are not orthogonal to each other but intersect at a lower (~ 80 deg) angle. This may be due to the relief of stresses on unloading and sectioning, and it may indicate that plane strain conditions were not present. Because of its flow characteristics, which are similar to those of metals, and because of its transparency, polycarbonate appears to be a good model material for the study of plastic flow initiated brittle fracture. It could be used to check the theoretical slip line field solutions proposed for a variety of loading conditions.

SEVERAL authors¹⁻¹¹ have postulated the existence of a critical normal stress criterion for brittle fracture. Accordingly brittle (often cleavage) fracture occurs in a material when the normal component of the stress reaches a certain critical value. This condition is schematically illustrated by the stress limited line of the fracture envelope proposed by Beeuwkes⁷ in Fig. 1. The value of the limiting fracture stress, σ_F^* , characteristic of a material is assumed to be independent of temperature and rate of loading,^{3,6} but may depend on the strain history.^{7,8}

In a tensile test, normal slip usually occurs at stress levels considerably lower than this critical stress σ_F^* and fracture is strain limited.^{7,8,12} When the test temperature is lowered, the observed occurrence of brittle fracture, predominantly in bcc metals and alloys, can be attributed to the increase of the yield strength. The stress triaxiality produced in the vicinity of notches and cracks also causes an increase in the yield stress due to plastic constraint. This increase can be calculated from Hill's slip line field theory.¹³ Under conditions of plane strain, neglecting strain hardening, the yield stress rises with increasing distance from the notch root towards the elastic-plastic interface. If that interface is at a distance b from the notch root of radius ρ along the x axis, the maximum normal stress in the y direction (loading direction) is given by

$$\sigma_y = 2k \left[1 + \ln \left(1 + \frac{b}{\rho} \right) \right] \quad [1]$$

Thus there exists a possibility for initiation of brittle fracture below the notch root at the elastic-plastic interface.

A. M. GARDE is Graduate Research Assistant, Department of Metallurgy and Materials Engineering, The University of Florida, Gainesville, Fla. 32601. V. WEISS is Professor of Materials Science, Department of Chemical Engineering and Materials Science, Syracuse University, Syracuse, N. Y. 13210.

Manuscript submitted June 14, 1971.

The critical fracture stress, σ_F^* , could be calculated from Eq. [1] if the yield strength of the material, $2k$, the notch root radius and the distance b from the notch root of the fracture origin were accurately known.

This is illustrated in Fig. 2. However, the value of

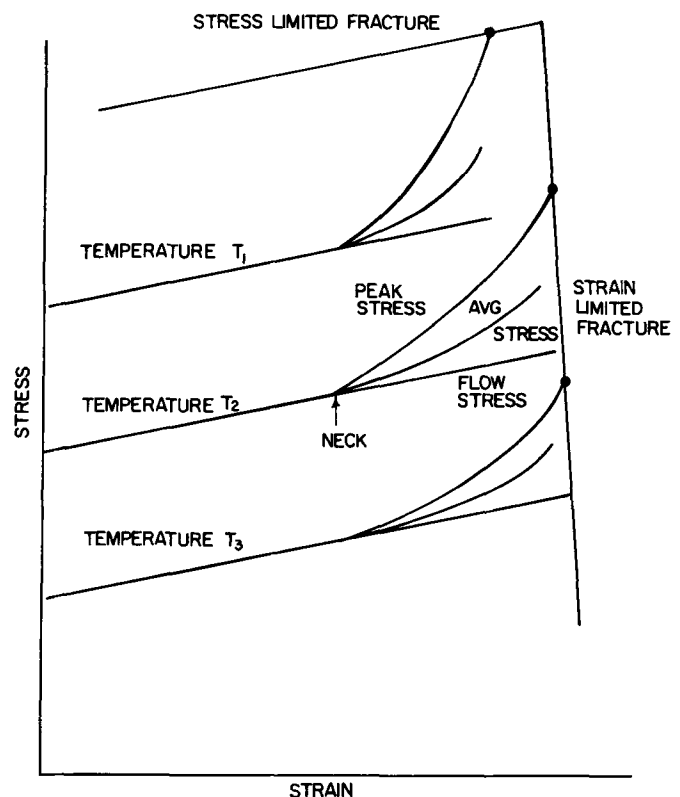


Fig. 1—Schematic illustration of Beeuwkes fracture criterion.^{7,8}

σ_F^* was found to depend on the notch root radius, weakly for mild notches and quite strongly for sharp notches.⁵

In order to calculate the maximum normal stress, researchers in this field used different methods to determine the stress distribution below the notch root. Hendrickson, Wood, and Clark³ have suggested using Allen and Southwell's relaxation method¹⁴ to determine the maximum stress for a special notch geometry. Beeuwkes^{7,8} has improved and extended slip line solutions to parabolic and elliptical notches and cracks. Hu¹⁵ has evaluated experimental results on pressure vessel steels with Beeuwkes' analysis and found good agreement. Green and Hundy¹⁶ have obtained plane strain slip line solutions for Izod and Charpy impact bend tests. Their estimates of yield point load agree well with experimental values. Wilshaw and Pratt¹⁷ have experimentally determined plane strain slip line fields around a Charpy notch by etching techniques. Griffis and Spretnak¹⁸ have used an etching technique to measure the plastic zone size below the notch in plane strain and compared it with theory.

Fracture origin studies were conducted by many workers both on fractured specimens and by metallographic examination of notched specimens loaded to a level below their failure load. Fractographic studies of broken specimens were carried out by Wilshaw¹⁹ on mild steel Charpy specimens. He found a discontinuity in the fracture profile below the notch root and suggested that this discontinuity was due to original cleavage cracks blunted by plastic deformation. Herrod, Hengstenberg, and Manjoine²⁰ have observed subsurface crack nucleation leading to fracture in beryllium WOL (wedge-opening-load) specimens on the metallographically polished face of the specimens.

Knott and Cottrell⁴ observed cleavage cracks in unbroken low carbon steel notch bend specimens in the plastically deformed region below the notch root. Recently Govila²¹ obtained longitudinal subsurface cracks in 3 pct silicon iron single crystals. These cracks were nucleated at small spherical nonmetallic inclusions and propagated along the cleavage plane, parallel to the loading direction.

The main problem in fractography is the difficulty of positively identifying the fracture origin. Many times fracture of brittle phases precede the fracture of the matrix under conditions that may be quite different from those required for nucleation of the domi-

nant fracture. Large shear deformations, *e.g.*, in the immediate vicinity of the notch root, are often sufficient to produce microcracks in brittle phases. Thus for inhomogeneous materials a concentration of microcracks in brittle phases may not represent the principal fracture origin.

Therefore positive evidence for brittle crack initiation by slip at the plastic-elasticity boundary below the notch root is still lacking. It was the objective of the present study to demonstrate the occurrence of slip initiated brittle fracture in polycarbonate.

Polycarbonate was chosen as a test material because:

1) The shape of its stress-strain curve is similar to that of a metal²² though polycarbonate is a non-crystalline polymer. Nevertheless plastic flow occurs as the result of the deviatoric component of the stress tensor.

2) Polycarbonate is transparent and can readily be sectioned and repolished to restore transparency so that subsurface cracks can be observed easily.

3) Plastic deformation reduces the transparency of polycarbonate (due to the formation of crazes which are plastic deformation zones in amorphous thermoplastics; they are spanned by stretched molecules)²²⁻²⁴ so that the macroscopic plastic zone and the elastic-plastic boundary in the vicinity of the stress concentration can be located easily.

It is, however, strongly emphasized that the material was chosen only as a model material and that it was not the purpose of the study to elucidate the plastic flow behavior of polycarbonate. The latter has been the subject of numerous studies.²²⁻²⁴ The fracture

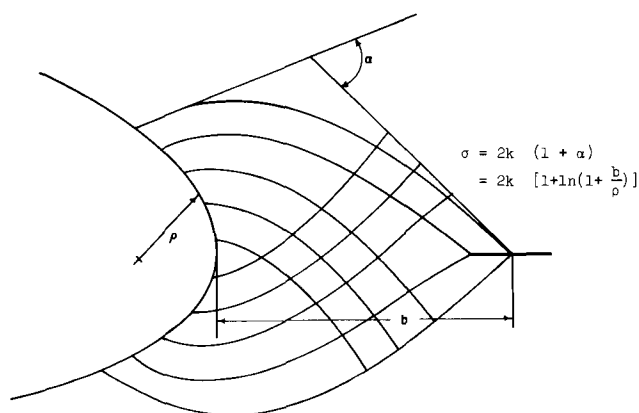


Fig. 2—Shear stress trajectories for a circular notch showing anticipated locus of brittle fracture nucleus at the elastic-plastic interface.

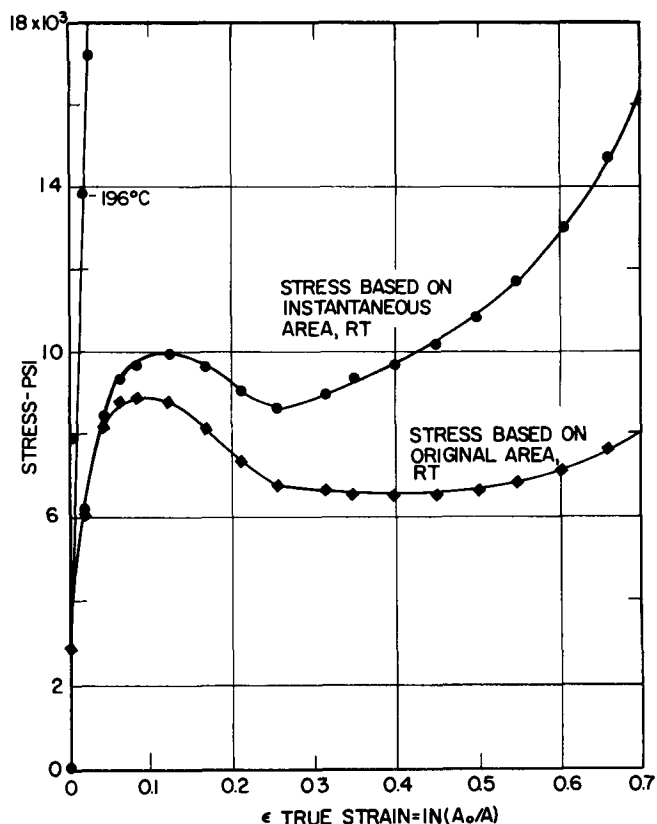


Fig. 3—Stress strain curve of polycarbonate at room temperature and -196°C (longitudinal strain based on diameter change).

experiments discussed here lie totally in the small plastic strain regime, where the analogy to metal behavior seems warranted.

EXPERIMENTAL PROCEDURE AND RESULTS

To determine the conventional mechanical properties of polycarbonate at different temperatures, smooth cylindrical specimens, of gage length 0.75 in. and gage diameter 0.25 in. were tested in tension on a 10,000 lb. capacity Instron machine at a crosshead speed of 0.02 in./min. Uniaxial tension tests were carried out at room temperature (25°C) and liquid nitrogen temperature (-196°C). The strain was determined by means of a diameter gage assuming volume constancy. At both temperatures the fracture surfaces were normal to the direction of the applied stress. At room temperature the stress strain curve of the specimen shows upper and lower yield points, Fig. 3. A neck develops, which on further loading, spreads over entire gage length unless fracture intervenes. Fracture occurred without the development of a second neck at a true stress of approximately 17,000 psi and a true strain of about 70 pct. At the temperature of -196°C, fracture occurred at a true stress of 24,000 psi and strain of 5 pct, Fig. 4.

The principal part of this investigation was conducted on double edge notched tension specimens of 0.5 in. thickness as shown in Fig. 5. From a series of preliminary tests, it was established that loading could be stopped rapidly enough upon the first appearance of subsurface cracks, before complete failure occurred. It was also established that a specimen thickness

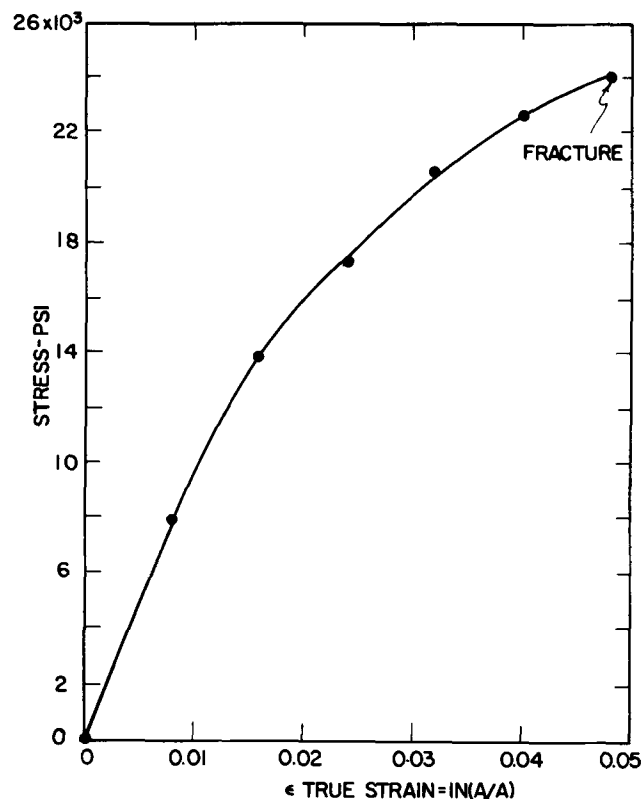


Fig. 4—Stress strain curve of polycarbonate at liquid nitrogen temperature (longitudinal strain based on diameter change measurement).

of 0.5 in. was necessary to prevent through-yielding and to obtain plane strain conditions at midthickness of the specimens. For the main program, three different notch root radii, 0.01, 0.005, and 0.001 in. with a notch angle of 60 deg were selected. To facilitate the observation of crack initiation below the notch root, the midportion of each specimen was polished using standard metallographic polishing techniques.

These polished specimens were loaded in tension at room temperature (25°C) on an Instron machine at a crosshead speed of 0.02 in./min. The load extension curve was recorded. While the specimen was being loaded, the portion immediately below the notch root was constantly observed for crack initiation directly and through a microscope. A high intensity mercury lamp was directed to give sufficient light to detect the subsurface cracks. As soon as the first crack formation was observed, the specimen was unloaded. All specimens were tested in this manner. Constant observation for crack initiation was necessary as once the crack was initiated, rapid crack growth and total failure followed quickly.

Each unbroken specimen was sectioned and polished for microscopic observation in an oblique direction as indicated in Fig. 5. A typical reflected light photograph, showing an oblique view of the notched section, is given in Fig. 6. The dark spots beneath the plastic regions below the notch root, show the initial cracks at approximately midthickness, at the elastic-plastic interface.

The specimen orientation was changed for microscopic observation in the normal direction as shown in Fig. 5. A typical photograph of the normal view, parallel to the tensile axis, *cf.* Fig. 5, using monochromatic (orange) polarized light is shown in Fig. 7. This figure shows crack initiation away from the notch root. The Newton rings generated by reflection from the two crack surfaces delineate the residual crack opening across the plane perpendicular to the direction of vision. The speckled region between the notch root and the crack is the plastic zone. The horizontal line separating bright and dark regions is the notch root.

To examine the plastic zone in more detail, a thin (thickness about 1 mm) longitudinal slice was cut from each specimen at midthickness. Each slice was examined microscopically in the transverse direction (in the thickness direction of the original specimen) as shown in Fig. 5, particularly the area in the vicinity of the notch root. Transverse photographs of slices taken

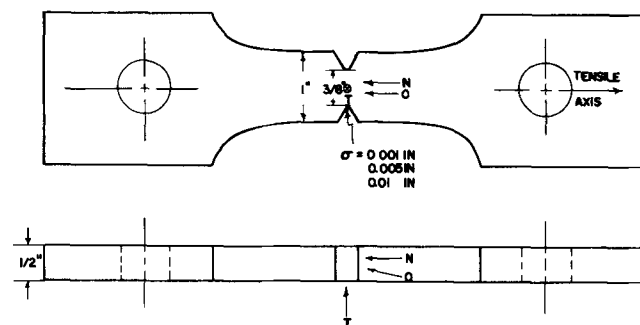


Fig. 5—Geometry of notch tension specimens. *O* ≡ direction of observation for fig. 6 (oblique view), *N* ≡ direction of observation for fig. 7 (normal view), *T* ≡ direction of observation for figs. 8 and 9 (transverse view).

from specimens with different notch root radii are given in Figs. 8 and 9. These pictures show slip lines in the plastic region, and crack nucleation away from the notch root, at the elastic-plastic interface. The locus of the ends of the slip lines gives an indication of the boundary of the plastic zone. Fig. 8 shows a transverse view for a notch root radius of 0.005 in. Though plane strain conditions appear to have been satisfied at the midthickness below the notch ($t/\rho > 50$, t is the thickness), the slip lines do not intersect orthogonally. The average angle of intersection is 81 deg. This discrepancy may be due to unloading and

sectioning of the specimen. Under load, the slip lines may well have been orthogonal to each other and the observed angle of intersection could be a result of the unloading strains, including release of residual stresses due to slicing. The angle of intersection of the slip lines observed by Wilshaw and Pratt¹⁷ was also less than 90 deg.

Fig. 9 shows a transverse view of a slice with a notch root radius of 0.001 in. Many off-axis cracks are seen to be initiated away from notch root, instead of a single crack as observed for larger root radii. This occurrence supports Beeuwkes' analysis of fracture

Fig. 6—Oblique view of fracture origins ahead of the notch, $\rho = 0.005$ in. Magnification 10 times.

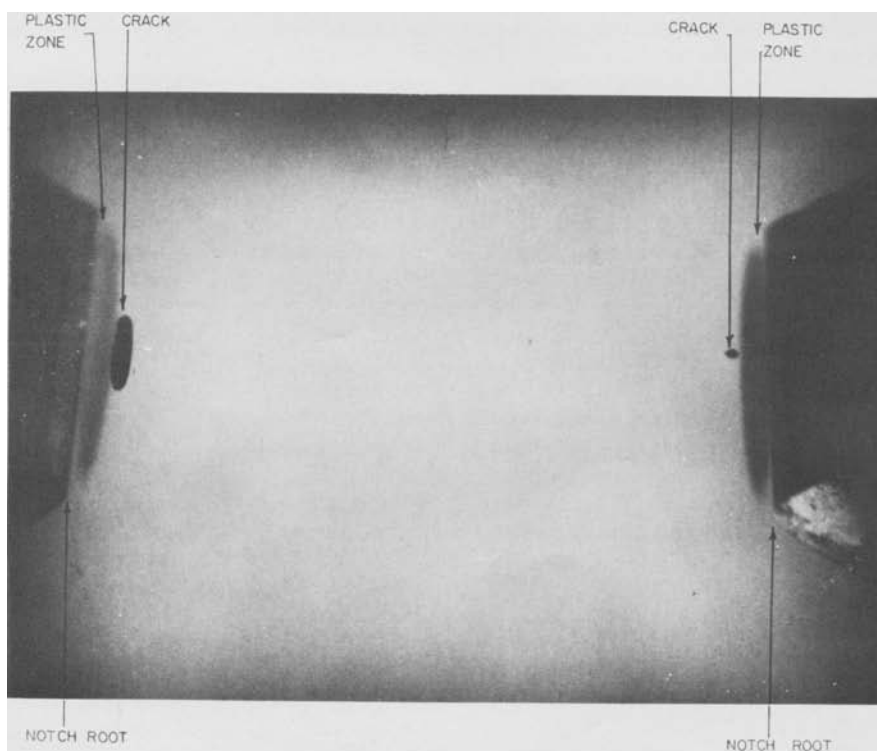
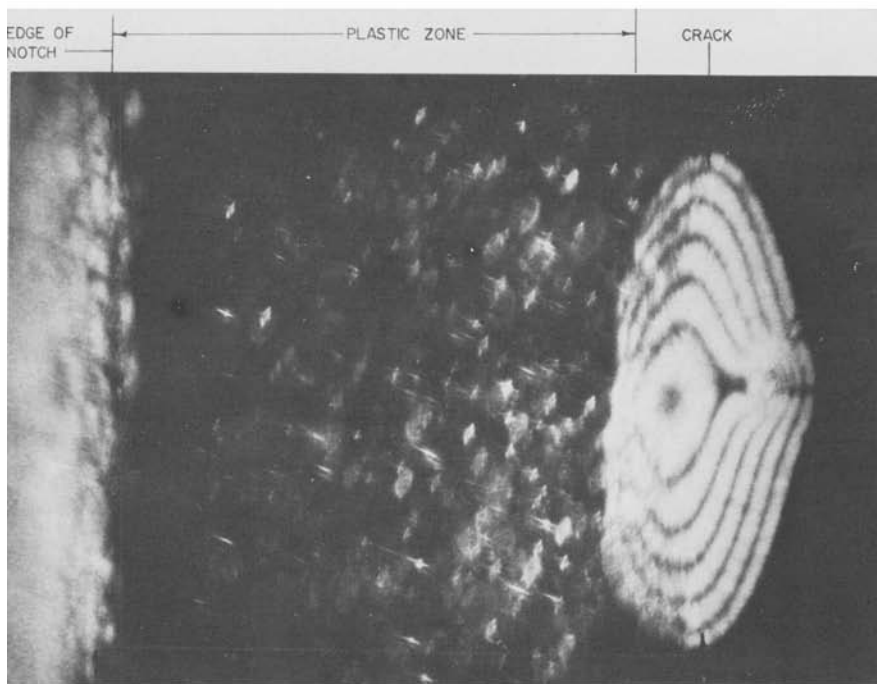


Fig. 7—Normal view of fracture origin ahead of the notch root, $\rho = 0.01$ in. polarized light. Magnification 85 times.



initiation near parabolic notches which predicts normal stress maxima at two points away from axis passing through the notch roots.

Similar tension tests on specimens with central holes of diameters 0.04 and 0.05 in. confirmed these findings and also showed crack nucleation at some distance from the hole.

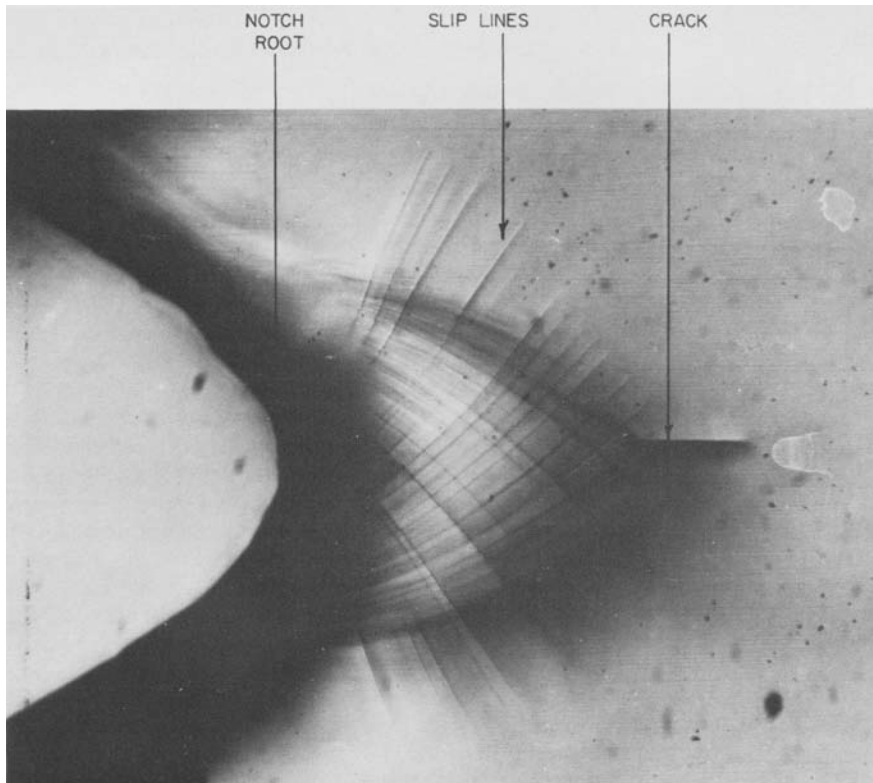


Fig. 8—Transverse view of midthickness slice showing fracture origin at elastic-plastic boundary and slip lines, $\rho = 0.005$ in. Magnification 195 times.

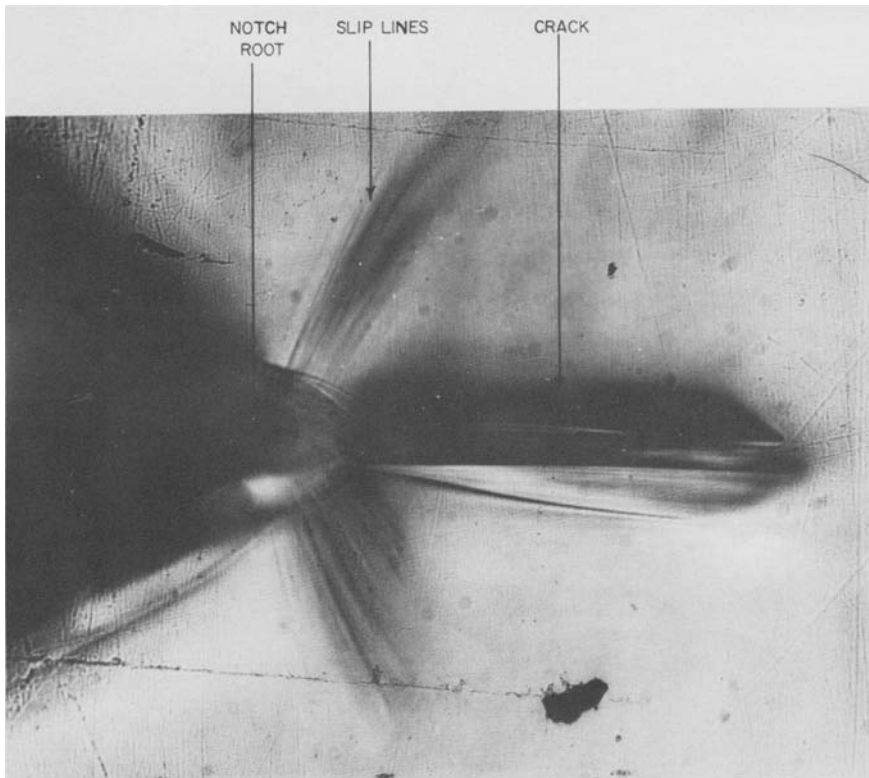


Fig. 9—Transverse view of midthickness slice showing many off axis cracks initiated at elastic-plastic interface and slip lines, $\rho = 0.001$ in. Magnification 270 times.

DISCUSSION

It is now possible to calculate the fracture stress σ_F^* from the yield strength $2k$ and the location of the fracture origin. It is difficult to define lower yield stress in polycarbonate as the yield phenomenon extends over a wide strain interval. Therefore in the present calculations, the stress at the pseudoplastic limit, 8700 psi, is used as lower yield stress. From Eq. [1], using the lower yield stress of the material, the fracture stress values for the various specimens are given below.

Table I

Root Radius ρ in.	Fracture Stress σ_F^* psi
0.001 <i>a</i>	21,800
0.005 <i>a</i>	21,400
0.01 <i>a</i>	20,600
0.02 <i>b</i>	11,400
0.025 <i>b</i>	11,100

a Double edge notched specimens
b Specimens with central holes.

The results for the double edge notched specimens are in close agreement and close to the tensile strength of polycarbonate at liquid nitrogen temperature.

Thus the results confirm the postulate of a constant normal fracture stress. For the specimens with holes, 0.02 and 0.025 in. radius the calculated fracture stresses lie in the range of 11,100 to 11,400 psi. These values are considerably below those for the notched specimens having smaller root radii. The discrepancy is attributed to the possibility that plane strain conditions may not be satisfied for these larger root radii.

Another method for determining the critical microscopic fracture stress σ_F^* , based on a parabolic crack shape has been proposed by Beeuwkes.⁸ In this theory the maximum shear stress trajectory angle change is related to a parameter L which is given by

$$L = \frac{Y}{S_N} \sqrt{\frac{\rho_F}{a}} + 2(1 - \mu^2) \frac{Y}{E} \quad [2]$$

where S_N is nominal stress; a , the notch depth; ρ_F , the notch root radius at fracture, μ , Poisson's ratio; E , Young's Modulus; and Y , the yield strength. The relation between L and maximum angle change, α , is tabulated by Beeuwkes, and it is also plotted.⁸

Assuming that the root radius does not change significantly after crack initiation below the notch, the value of L can be calculated for each specimen. The values of α are obtained from Beeuwkes' graph.⁸ Substituting this value of maximum angle change α into $\sigma_{\max} = 2k(1 + \alpha)$ the maximum tensile stress below the notch root is obtained. The results are shown in the table below.

Accordingly the critical tensile stress values vary from 20,300 psi to 23,500 psi. The fact that these values are higher than those computed for circular notches, Eq. [1], is not surprising, as Beeuwkes' analysis applies to parabolic notches. For sharp notches, the parabolic crack approximation may be more appropriate as shown by the occurrence of off-axis cracks in the specimen with $\rho = 0.001$ in., Fig. 9.

Table II

ρ in	S_N psi	L	α -Radian	σ_F^* psi
0.001	4660	0.23	1.35	23,500
0.005	4320	0.38	1.08	20,800
0.01	5920	0.41	1.03	20,300

$a = 0.3125$ in.

Y for polycarbonate = $1.15 \times 8700 = 10,000$ psi (Assuming von Mises yield criterion).

E for polycarbonate = 160,000.

CONCLUSIONS

From the results of the study, the following conclusions can be drawn:

1) Cracks nucleate at the elastic-plastic boundary. The local normal stresses at crack nucleation calculated from slip line field theory are approximately constant and independent of notch geometry for notch root radii 0.001, 0.005, and 0.01 in. The calculated values of the fracture stress are 21.2 ± 0.6 ksi. This variation is considered within the experimental accuracy and hence the critical normal stress theory for fracture appears applicable to polycarbonate. Assuming parabolic notch shapes, the fracture stresses can be calculated from Beeuwkes' theory and are found to be 21.5 ± 2.0 ksi. The true fracture stress of a smooth tensile specimen at liquid nitrogen temperature is 24 ksi. The stresses for crack nucleation near central holes with 0.04 and 0.05 in. diam were found to be much lower, 11.2 ± 0.2 ksi. This is probably due to a loss of plane strain conditions.

2) Single cracks are nucleated on the axis passing through the notch root for the root radii 0.01 in. and 0.005 in. However, for the specimen with notch root radius 0.001 in. many off-axis cracks are found. Beeuwkes' theory of parabolic cracks predicts two stress maxima away from the axis. Hence the parabolic crack approximation may be more appropriate for notch root radii less than 0.005 in.

3) Polycarbonate develops slip lines which can be used to check the theoretical predictions. The slip lines observed on the midthickness slices do not intersect orthogonally. This may be due to a loss of plane strain conditions, particularly after slicing, and also to stress relaxation on unloading and slicing.

ACKNOWLEDGMENT

This work was sponsored by the United States Army Research Office under Contract No. DA-31-124-ARO-(D)-112. The authors are indebted to Dr. Rainier Beeuwkes for his interest and encouragement.

REFERENCES

1. Lame Navier: *Paris Mem. Par. Divers Savants*, 1833, t-4.
2. P. Ludwik: *Elemente der Technologischen Mechanik*, Berlin, 1909.
3. J. A. Hendrickson, D. S. Wood, and D. S. Clark: *Trans. ASM*, 1958, vol. 50, p. 656.
4. J. F. Knott and A. H. Cottrell: *J. Iron Steel Inst.*, 1963, vol. 201, p. 249.
5. A. S. Tetelman, T. R. Wilshaw, and C. A. Rau, Jr.: *Proc. Int. Symp. on Fracture Mechanics*, Kiruna, Sweden, August 1967.
6. J. A. Hendrickson, D. S. Wood, and D. S. Clarke: *Trans. ASM Soc. Met.*, 1959, vol. 51, p. 629.
7. R. Beeuwkes, Jr.: *Proc. of the Third Sagamore Conf. on Materials Evaluation in Relation to Component Behavior*, 1956, p. 89.

8. R. Beeuwkes, Jr.: *Surfaces and Interfaces*, Syracuse University Press, vol. II, 1968.
9. J. F. Knott: *J. Iron Steel Inst.*, 1966, vol. 204, p. 104.
10. J. F. Knott: *J. Iron Steel Inst.*, 1967, vol. 205, p. 966.
11. V. Weiss: in *Fracture an Advanced Treatise in Seven Volumes*. vol. III, H. Liebowitz, ed., p. 34, Academic Press, 1970.
12. R. Chait: Ph.D. Dissertation, Syracuse Univeristy, March 1967.
13. R. Hill. *Mathematical Theory of Plasticity*, Oxford, London, 1950.
14. D. N. de G. Allen and Sir. R. Southwell *Royal Soc., London, Phil. Trans.*, 1949, Series A, vol. 242, p. 379.
15. W. Hu: M. S. Thesis, Syracuse University, March 1969.
16. A. P. Green and B. B. Hundy: *J. Mech. Phys. Solids*, 1956, vol. 4, p. 128.
17. T. R. Wilshaw and P. L. Pratt: *J. Mech. Phys. Solids*, 1966, vol. 14, p. 7.
18. C. A. Griffis and J. W. Spretnak: Ohio State University Research Foundation Technical Report AFML-TR-68-269, October 1968.
19. T. R. Wilshaw *J. Iron Steel Inst.*, 1966, vol. 202, p. 936.
20. D. L. Herrod, T. F. Hengstenberg, and M. J. Manjoine: *J. Mater. JMLSA*, 1969, no. 3, vol. 4, p. 618.
21. R. K. Govila: *Acta Met.*, 1969, vol. 17, p. 1209.
22. G. Jacoby and C. Cramer: Tech. Report No. 47, Institute for the Study of Fatigue and Reliability, Columbia University, April 1967.
23. R. P. Kambour: *Polym.*, 1964, vol. 5, p. 143.
24. G. Menges and H. Schmidt: *Plast. Pym.*, Feb. 1970, p. 13.